01 Jan 2022

Early Wildfire Detection using Uavs Integrated with Air Quality and Lidar Sensors

Doaa Rjoub

Ahmad Alsharoa
Missouri University of Science and Technology, aalsharoa@mst.edu

Ala'Eddin Masadeh

Recommended Citation

D. Rjoub et al., "Early Wildfire Detection using Uavs Integrated with Air Quality and Lidar Sensors," *IEEE Vehicular Technology Conference*, Institute of Electrical and Electronics Engineers, Jan 2022.
The definitive version is available at https://doi.org/10.1109/VTC2022-Fall57202.2022.10012938

Early Wildfire Detection using UAVs Integrated with Air Quality and LiDAR Sensors

Doaa Rjoub[1], Ahmad Alsharoa[1], and Ala'eddin Masadeh[2]
[1]Missouri University of Science and Technology, Rolla, Missouri, United States,
Email: {drjoub, aalsharoa}@mst.edu
[2]Al-Balqa Applied University, Salt, Jordan,
Email: amasadeh@bau.edu.jo

2022 IEEE 96th Vehicular Technology Conference (VTC2022-Fall) | 978-1-6654-5468-1/22/$31.00 ©2022 IEEE | DOI: 10.1109/VTC2022-Fall57202.2022.10012938

***Abstract*— Every year, wildfires burn out countless hectares of lands, resulting in ecological, environmental, and economic damage. This paper presents an energy management system that consists of an unmanned aerial vehicle (UAV) equipped with air quality and light detection and ranging (LiDAR) sensors for monitoring forests and recognizing flames early. We develop a novel approach for autonomous patrolling system. This approach has the advantage of effectively detecting wildfire incidents, while optimizing the energy consumption of the UAV's battery to cover large areas. When a wildfire is detected, the UAV is able to transmit real-time data, such as sensor readings and LiDAR data, to the nearby communication tower. We formulate an optimization problem that minimizes the overall UAV's energy consumption due to patrolling. Based on the pollutant dispersion mode, we propose a novel UAV patrolling solution based on genetic algorithm with the goal of maximizing the patrolling coverage of the UAV taking into account the UAV's battery constraints. More specifically, we optimize the UAV's flight path using a plume dispersion model to find the concentration of common gases of wildfire. Finally, simulations are presented to show the efficiency and validity of the solution.**

I. Introduction

The severity and quantity of wildfires have grown considerably in the previous decade around the world [1]. In the United States (U.S.) only, over 8.7 million acres were burned in 2018, costing approximately 24 billion dollars in infrastructure damage and firefighting. Latest forest fires in Western United States and Australia have engulfed various states, burning areas greater than 50 million acres [1]. The severity and frequency of wildfires, as well as the hazards connected with them, are predicted to rise in the future as a result of climate change [2].

The traditional approach of wildfire detection employs lookout stations located in high-visibility areas [3]. This system is labor intensive and has difficulties with worker safety [3]. Furthermore, this strategy may cause a delay in the detection of a fire (i.e, slowness in noticing or reporting the incident). Wildfire detection and forest fire monitoring may also be accomplished via satellite remote sensing [4]. It can locate current flames, assess burnt regions, and evaluate fire emissions [5]. However, satellite imaging has a low spatial resolution (tens of meters) and needs a cloud-free observation region, making it challenging to recognize wildfires in their early stages [6]. Another approach for fire detection and monitoring is thermal imaging [7], which may be used to locate hotspots during the mapping and evolution of a fire. However, thermal cameras have low spatial resolution and are susceptible to weather influence, as the thermal signal coming from the fire may be blocked by thick canopies [7].

Air quality detection, particularly tracers of wildfire emissions, can be useful in recognizing wildfire outbreaks. These sensors are inexpensive and sensitive to the species being examined [8]. In general, air quality sensors operate in three stages. In the first stage, the sensors radiate particles in the air via laser scattering. In the second stage, the sensors then capture the light scattered over time. Finally, the sensors calculate the concentration, diameter, and number of the particles using their build-in microprocessors. For example, air quality Particulate Matter (PM) sensors can map the spatio-temporal distribution by utilizing Kriging interpolation approach [9]. Other sensors such as low cost Carbon Monoxide (CO) sensors that are based on triboelectric nanogenerators are available that are able to monitor CO contents without a battery via harvesting tree branch movement [10]. However, one issue with employing air quality sensors in detecting wildfire is requiring a large number of sensors if they are placed at fixed sites. Moreover, deploying these sensors in hazardous places or woods is problematic.

Due to their low cost, minimal maintenance, high mobility and wide coverage area, including danger areas, unmanned aerial vehicles (UAVs) have become a practical and feasible solution for wildfire detection and forest management (i.e., it can work in regions that people cannot access or that are out of sight) [11]–[14]. In [15], the authors proposed a vision-based UAV system that processes collected photos using color and motion features. However, this method has a negative effect of the canopy and weather conditions. In this paper, we design a novel energy-efficient UAV patrol system for the early wildfire detection based on the pollutant dispersion model. Further, we propose to integrate the air quality sensors (PM and CO sensors) with light detection and ranging (LiDAR) sensor [16]. LiDAR is characterized by its capability of producing 3D real-time maps of pollutant concentrations by emitting several laser beams throughout a field-of-view (FoV) region and measuring the distance between the sensor and the item the laser beams strike. Because LiDAR sensors generate large amounts of data during scanning their surroundings, the UAV will only send the LiDAR data when the measured contaminants by conventional air quality sensors exceed specified thresholds. This will reduce the amount of data sent from the LiDAR

sensors and allow the communication tower to process the data faster. The key contributions of this work can be summarized by:

II. System Model

We consider a single UAV that patrols over a flat, rectangular forest area for a wildfire detection. The UAV is provided by a radio transceiver that allows it to exchange data with a nearby communication tower if a wildfire is detected. The wind direction in the region is defined by θ_w (the north is indicated by $\theta_w = 0$ as a reference). The UAV has LiDAR and air quality sensors to track PM (μgm^{-3}) and CO (ppm) levels. We assume that a wildfire incident is recognized if the measured concentrations of air pollutants by both sensors (i.e., PM and CO sensors) exceed the forest threshold backgrounds [17]. When this happens, the UAV sends real-time sensor readings and LiDAR data to the nearby communication tower.

An early-stage wildfire can occur at a random point in the patrolled region and constantly released PM and CO pollutants into the environment via a plume that was carried by the wind and scattered in all directions. Let the speed of the UAV be V; therefore, $V\hat{T}$ is the maximum distance the UAV may fly during each time slot t, where $\hat{T}$ denotes the duration of the time slot. The UAV's location is represented as 3D coordinates within a time period t as $\hat{U}[t] = (x[t], y[t], z[t])$. The following parameters are optimized for successful wildfire detection and reporting (1) the UAV's altitude to guarantee that the UAV can pass through the plume, and (2) the flight pattern of the UAV that ensured the UAV samples were in the plume for a considerable time.

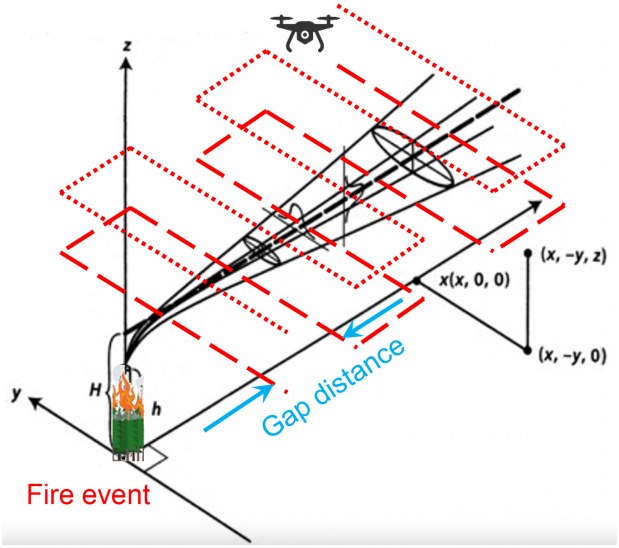

Fig. 1: A schematic diagram of GDM for predicting the air pollutants concentrations in a plume.

A. Pollutant Dispersion Model

Dispersion models are commonly used to describe plume transfer [18]. The Gaussian dispersion model (GDM), as shown in Fig. 1, is the most extensively used model for predicting the movement of air contaminants in a plume, where the concentration of air contaminants released from a source can be measured by [18]:

$$C(x,y,z) = \frac{Q}{2\pi u \sigma_y(x)\sigma_z(x)} \exp\left(-\frac{y^2}{2\sigma_y^2(x)}\right). \left[\exp\left(-\frac{(z-H)^2}{2\sigma_z^2(x)}\right) + \exp\left(-\frac{(z+H)^2}{2\sigma_z^2(x)}\right)\right] \quad (1)$$

where C denotes the steady-state concentration at location (x, y, z), Q indicates the emission rate, and the horizontal and vertical spread parameters are denoted by $\sigma_y(x)$ and $\sigma_z(x)$, respectively, depending on the atmospheric stability and distance x. Note that z indicates the vertical distance from the plume center line, and u is the average wind speed, and H represents the emission point's effective height. For ease of usage, we will denote the PM and CO indices as $i = \{1, 2\}$, respectively. Equivalently, sensor concentrations of PM and CO, are denoted as C_1 and C_2, respectively. The binary variable $\rho_i[t]$ is designated to show whether the concentration of pollutant i exceeds the concentration threshold $C_{th,i}$ during period t:

$$\rho_i[t] = \begin{cases} 1, & \text{if } C_i[t] \geq C_{th,i} \text{ during time slot } t \\ 0, & \text{otherwise.} \end{cases} \quad (2)$$

By defining $\bar{C}_i$ as the maximum level of the pollutant concentration i, the value that can be measured precisely at the point of fire, (2) can be written as:

$$(C_{th,i} - C_i[t]) - \bar{C}_i(1 - \rho_i[t]) \leq 0, \quad \forall i, \forall t, \quad (3)$$

and

$$(C_i[t] - C_{th,i}) - \bar{C}_i \rho_i[t] \leq 0, \quad \forall i, \forall t. \quad (4)$$

It should be noted that using both constraints (3) and (4) are required to express (2) in mathematical formulas. Suppose $\rho[t] = \rho_1[t] = \rho_2[t]$, where $\rho[t]$ equals 1 if both pollutants' concentrations are higher than the concentration threshold and 0 otherwise (i.e., one pollutant concentration is below the threshold).

We assume that wildfire is identified when both PM and CO concentrations exceed their respective concentration thresholds. As a result, the UAV must broadcast real-time data to the he nearby communication tower. Based on quality-of-service (QoS), which is presented as a data rate threshold. We assume that, in addition to air-quality sensors reading, the UAV can transmit LiDAR data that deliver 3D detailed maps to improve decision accuracy. It is worth mentioning that the QoS of sensor readings differs from the QoS of LiDAR 3D maps. It also should be noted that different QoS data are referred to as a distinct data types.

The main objective is to send all data types to the chosen BS when the concentrations of PM and CO pollutants exceed the specified threshold (i.e., $\rho[t] = 1$).

B. UAV Energy Model

Denote the total communication power for transmission during the t-th time slot is $P_C[t]$. In addition to transmission power, the UAV uses flying and hovering powers $P_F[t]$, which are denoted as [19]:

$$P_F[t] = \left(\sqrt{\frac{(m_{\text{tot}}G)^3}{2\psi r_p^2 \omega_p \psi}} + P_s \right) \tag{5}$$

where P_s represents the amount of power consumed by the UAV equipment in (W), ψ denotes the air density in (kg/m^3), and m_{tot} represents the mass of the UAV in (kg). The UAV's propellers' number and radius are indicated by the parameters ω_p and r_p, respectively. Thus, the overall consumed energy may be expressed as follows:

$$E_{tot} = E_F + E_C = \hat{T} \sum_{t=1}^{T} P_F[t] + \hat{T} \sum_{t=1}^{T} P_C[t]. \tag{6}$$

Note that since $E_F >> E_C$ (in contrary to transmission, power which uses only fractional Watts, flight uses several Watts), the approximate total energy in (6) is given by:

$$E_{tot} \approx E_F = \hat{T} \sum_{t=1}^{T} P_F[t], \tag{7}$$

where T is a dependent variable that has an impact on the overall amount of energy; for instance, if the patrol UAV completes the patrol flying trip earlier, then T gets smaller and the energy is reduced.

III. Problem Formulation

This section develops the mathematical formulation for the UAV patrolling problem. The objective is to minimize the overall consumed energy and meet the detection threshold, and budget for UAV battery. The goal is to identify the optimal UAV trajectory inside a given region. The energy consumption of the UAV can be minimized by minimizing the flight time of the UAV when it reaches $C_{th,i},\ \forall i = \{1, 2\}$ and detects wildfire. This may be accomplished by optimizing the trajectory of the UAV. Due to the limited capacity of the UAV battery, the UAV's flight path limits the area that the UAV may patrol. For the sake of simplicity, let us assume that the UAV follows a rectangular track. Therefore, the horizontal gap distance between the two parallel legs which is given by Δx has a significant impact on the UAV's overall distance flown. A greater spacing results in inefficient wildfire tracer detection and reduced energy use, whereas a smaller gap results in longer flight distances and quicker battery usage. It should be noted that this Δx-optimized rectangular track might be simply changed to fit different tracks, such square or spiral tracks. For ease of use, the rectangular track was selected.

In this context, the maximum gap distance of the UAV is calculated using GDM. The longest distance the UAV could go and the size of the forest that could be patrolled are determined by the battery capacity of typical UAVs. To efficiently identify early-stage fire occurrences, the UAV's height and trajectory must be optimized. Consequently, the patrolling optimization problem can be expressed as

$$\underset{(z[t],y[t],\Delta x,)\geq 0,}{\text{minimize}} \quad E_{tot} \tag{8}$$

subject to

$$C(x = \Delta x, y[t], z[t]) \geq C_{th,i}, \quad \forall i, \tag{9}$$

where (9) constraint is used to guarantee that the horizontal spacing is Δx, and $z[t]$ considers meeting $C_{th,i}$ for both PM and CO pollutant species in the event that a wildfire occurs in the region of interest. This will make sure that any wildfires in the region of interest are detected. It should be noted that the $\rho[t]$ value will be dependent on a real-time concentration measurement of PM and CO sensors.

IV. UAV Patrolling Solution

In this section, we present our proposed UAV patrolling solution. In order to maximize the coverage area for the UAV patrols and to take into account the UAV's battery constraints. According to [18], the UAV must transverse the plume at the height of the plume centerline $z[t] = H$ in order to efficiently identify early-stage fire incidents. The formula used for calculating H is given by [18]:

$$H = h_0 + \frac{\nu_s d_s}{u} \left[1.5 + 2.68 \times 10^{-2} P_a . \left(\frac{K_s - K_a}{K_s} \right) d_s \right] \tag{10}$$

where h_0 is the height of the burning plume, ν_s is its upward velocity, d is its diameter at the emission point, P_a is its pressure, K_s is its temperature, and K_a is the temperature of the surrounding air. Additionally, as shown in Figure **??** the peak incidence will occur when $y = 0$ according to GDM. As a result, using [20], based on the surrounding environment and the available data describing fire plumes, the rectangular UAV motion's ideal or maximum horizontal spacing distance Δx can be determined by solving the following optimization problem. Note that minimizing E_F is equivalent to maximizing of Δx:

$$\underset{\Delta x}{\text{maximize}} \quad \Delta x \tag{11}$$

subject to:

$$C(x = \Delta x, y = 0, z = H) \geq C_{th,i}, \quad \forall i, \tag{12}$$

where the purpose of constraint (12) is to ensure that the horizontal spacing Δx fulfills $C_{th,i}$ for all polluting types (i.e., PM and CO). The optimization problem stated in (11)-(12) is non-convex and non-linear. Consequently, it is challenging to find the optimal solution, according to [21]. Due to its quick deployment and short convergence time, we propose using a meta-heuristic technique based on genetic algorithm (GA) to identify a nearly optimal path for patrolling horizontal gaps [22]. This method is primarily based on natural-random evolution. GA begins with creating a random set of population with a predetermined amount of strings. Strong strings survive the algorithm generation after generation, whereas weak strings die. Following that, the GA use mutation and crossover processes to build new strings from the surviving ones [22]. It should be noted that the crossover process consists of randomly splitting two surviving parent strings, and swapping the acquired pieces to form 2 new strings. The mutation operator, on the other hand, is used by changing a random string value with a particular probability [23].

V. Simulation Results

This section illustrates selected simulation results to demonstrate the benefits of the proposed patrolling approach. We take into account the reference emission rates $Q_{0,i}$ of PM and CO that follow, respectively, Gaussian distributions $\mathcal{N}(17.4, 7.2)$

and $\mathcal{N}(64.5, 16.7)$ [17]. $C_{th,1}$ and $C_{th,2}$ are assumed to be 75μg/m^3 and 150ppm respectively (in view of three times of the controlled concentration to recognize the fire occasion) [18], [24]. Table I provides a summary of the remaining simulation settings [18], [25]. Based on the dispersion model presented in (1), two stability scenarios (very unstable and neutral) are taken into consideration. In other words, σ_y and σ_z are determined in light of sensible approximated fit and given, respectively, as [18]:

$$\sigma_y = ax^b, \tag{13}$$

$$\sigma_z = cx^d + f, \tag{14}$$

where Table II lists the parameters a, b, c, d, f. Examples of a 2D Gaussian pollutants concentrations dispersion model in a plume for very unstable and neutral atmospheric stability conditions are shown in Figure 2-Figure 3, respectively .

Table I: Patrolling simulation parameters [18].

Constant	Value	Constant	Value	Constant	Value
V [m/s]	5	h_0 [m]	15	v_s [m/s]	1.55
d_s [m]	4.75	K_a [K]	308.15	K_s [K]	1106.15
P_a [mb]	1000	P_s [W]	0.5	m_{tot} [kg]	1
ψ [kg/m^3]	1.225	ω_p	4	r_p	0.2

Figure 4 depicts the horizontal gap Δx as a function of wind speed u. It is demonstrated that when the wind speed rises, the horizontal gap of all the various stability factors decreases. This is due to the inverse proportional relationship between pollutant concentration C and wind speed u is inverse propositional, as shown in (1). It is noteworthy that as C rises at the same position (x, y, z), so does Δx rise since the UAV can detect the C_{th} beyond this point. At low wind speed levels, the differences among various kinds of stability conditions are substantial. When $u = 20$[m/s], for example, Δx for neutral and severely unstable conditions are roughly 220m and 160m, respectively, with an estimated difference of 80m. When $u = 2$[m/s], Δx for neutral and severely unstable conditions are about 880m and 400m, respectively, with approximately 500m difference. As u rises, the distance between the various stability scenarios decreases.

Table II: Stability coefficients based on the GDM.

Stability	a	b	$\Delta x \leq 1$ km			$\Delta x > 1$ km		
			c	d	f	c	d	f
V.Unstable	213	0.894	440.8	1.941	9.27	459.7	2.094	-9.6
Neutral	68	0.894	33.2	0.725	-1.7	44.5	0.516	-13.0

Figure 5 shows the relationship between the horizontal gap Δx and the emission rate factor κ. As specified by the formula $Q_i = \kappa_i Q_{0,i}$, $\forall i = \{1, 2\}$, the parameter κ is used to represent the emission rate in terms of the reference emission rate. Notice that the emission rate factors for PM2.5 and CO are indicated by the symbols κ_1 and κ_2, respectively. This can demonstrate how the horizontal gap is affected by increasing or decreasing emission rates. According to Figure 5, the horizontal gap grows as κ increases for the same emission rate factor $\kappa = \kappa_1 = \kappa_2$. The proportional relationship between C and Q in (1) was thus validated. Therefore, when Q increases, Δx also increases.

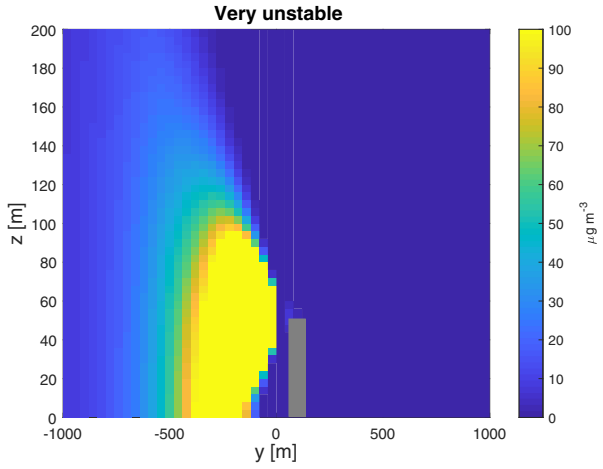

Fig. 2: 2D Gaussian pollutants concentrations dispersion model in a plume for very unstable stability situation.

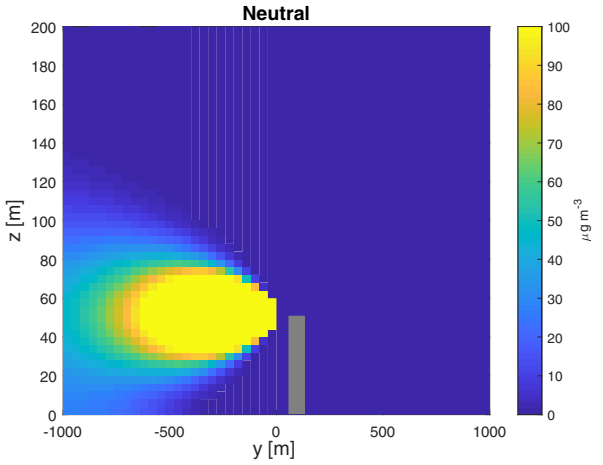

Fig. 3: 2D Gaussian pollutants concentrations dispersion model in a plume for neutral stability situation.

VI. Conclusion

This work proposed a unique approach for integrating UAVs with air quality and LiDAR sensors, as well as communication transceivers, to identify wildfires early. This developed framework can outperform thermal imaging and other current methods by detecting pollutants rapidly, recognizing the source of the fire, and providing more information about pollutant dispersion. Moreover, the concept of autonomous patrol optimization (i.e., optimizing the flight route of the UAV) can identify wildfire incidents effectively, while maintaining the UAV battery for a broader coverage area. This will result in a more reliable and energy-efficient wildfire detection approach. Future and active work will adopt novel approaches

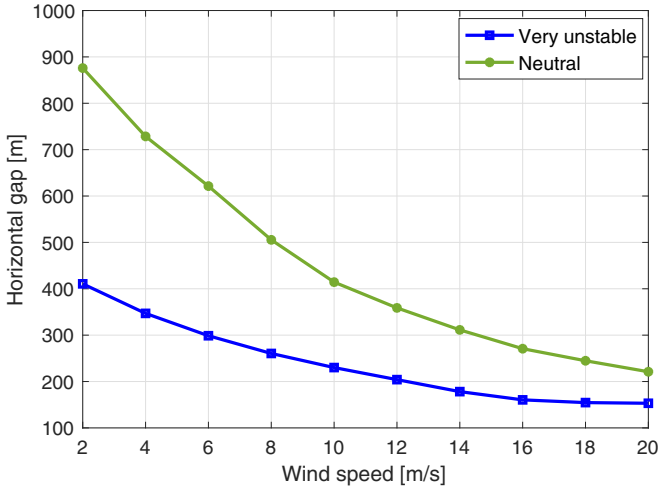

Fig. 4: The horizontal gap as a function of wind speed for different stability situations.

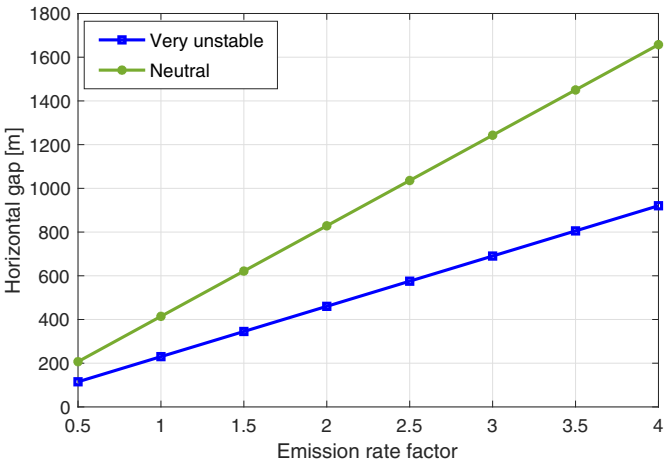

Fig. 5: The horizontal gap versus emission rate factor for different stability situations.

to develop new strategies that lead to enhance the performance of the systems. One idea is to explore several wildfire hotspot regions. These regions may be identified using historical data, and it is worthwhile to patrol the UAV above these hotspot regions in spirals or other motion patterns. This will come at the cost of increased UAV energy consumption and increased track complexity.

REFERENCES

[1] D. Kolaric, K. Skala, and A. Dubravic, "Integrated system for forest fire early detection and management," *Periodicum Biologorum*, vol. 110, pp. 205–211, 2008.

[2] Center for Climate and Energy Solutions, "Record wildfires push 2018 disaster costs to $91 billion," 2019. Available [online]: https://www.c2es.org/2019/02/record-wildfires-push-2018-disaster-costs-to-91-billion.

[3] A. Murray, "Optimising the spatial location of urban fire stations," *Fire Safety Journal*, vol. 62, pp. 64–71, 2013.

[4] S. Bao, N. Xiao, Z. Lai, H. Zhang, and C. Kim, "Optimizing watchtower locations for forest fire monitoring using location models," *Fire Safety Journal*, vol. 71, pp. 100–109, January 2015.

[5] Environment and Natural Resources, "Detecting wildfire," accessed 2021. Available [online]: https://www.enr.gov.nt.ca/en/services/wildfire-operations/detecting-wildfire.

[6] Z. Gao, L. Zhang, X. Li, M. Liao, and J. Qiu, "Detection and analysis of urban land use changes through multi-temporal impervious," *Journal of Remote Sensing*, vol. 14, pp. 593–606, 2010.

[7] J. Pardo, W. Aguilar, and T. Toulkeridis, "Wireless communication system for the transmission of thermal images from a UAV," in *Proc. of Conference on Electrical, Electronics Engineering, Information and Communication Technologies (CHILECON), Pucon, Chile*, October 2017, pp. 1–5.

[8] J. Hofman, M. E. Nikolaou, T. Huu Do, X. Qin, E. Rodrigo, W. Philips, N. Deligiannis, and V. P. La Manna, "Mapping air quality in iot cities: Cloud calibration and air quality inference of sensor data," in *2020 IEEE SENSORS*, 2020, pp. 1–4.

[9] J. Li, H. Li, Y. Ma, Y. Wang, A. Abokifa, C. Lu, and P. Biswas, "Spatiotemporal distribution of indoor particulate matter concentration with a low-cost sensor network," *Building and Environment*, vol. 127, pp. 138–147, January 2018.

[10] Y. Pang, S. Chen, J. An, K. Wang, Y. Deng, A. Benard, N. Lajnef, and C. Cao, "Multilayered cylindrical triboelectric nanogenerator to harvest kinetic energy of tree branches for monitoring environment condition and forest fire," *Advanced Functional Materials*, vol. 30. no. 32, pp. 207–2016, June 2020.

[11] D. Kinaneva, G. V. Hristov, J. Raychev, and P. Zahariev, "Early forest fire detection using drones and artificial intelligence," in *Proc. of the 42nd International Convention on Information and Communication Technology, Electronics and Microelectronics (MIPRO), Opatija Croatia*, May 2019, pp. 1060–1065.

[12] A. Alsharoa and M. Yuksel, "UAV-Direct: Facilitating D2D communications for dynamic and infrastructure-less networking," in *in Proc. of the 4th ACM Workshop on Micro Aerial Vehicle Networks, Systems, and Applications, Mobile Systems, Applications, and Services (MobiSys), Munich, Germany*, June 2018, pp. 57–62.

[13] M. Y. Selim, A. Alsharoa, and A. E. Kamal, "Short-term and long-term cell outage compensation using UAVs in 5G networks," in *Proc. of the IEEE Global Communications Conference (GLOBECOM), Abu Dhabi, United Arab Emirates*, Dec. 2018, pp. 1–6.

[14] F. Nait-Abdesselam, A. Alsharoa, M. Y. Selim, D. Qiao, and A. E. Kamal, "Towards enabling unmanned aerial vehicles as a service for heterogeneous applications," *Journal of Communications and Networks*, vol. 23, no. 3, pp. 212–221, June 2021.

[15] C. Yuan, Z. Liu, and Y. Zhang, "Aerial images-based forest fire detection for firefighting using optical remote sensing techniques and unmanned aerial vehicles," *Journal of Intelligent and Robotic Systems*, vol. 88, p. 635–654, January 2017.

[16] M. C. Lucic, H. Ghazzai, A. Alsharoa, and Y. Massoud, "A latency-aware task offloading in mobile edge computing network for distributed elevated LiDAR," in *Proc. of the IEEE International Symposium on Circuits and Systems (ISCAS), Seville, Spain*, 2020, pp. 1–5.

[17] F. Reisen, C. Meyer, C. Weston, and L. Volkova, "Ground-based field measurements of pm2.5 emission factors from flaming and smoldering combustion in eucalypt forests," *Journal of Geophysical Research: Atmospheres,*, vol. 123, no. 15, pp. 8301–8314, Aug. 2018.

[18] Cooper C. David and F.C. Alley, *Air pollution control : A design approach*. Waveland Press Inc., September 2010.

[19] D. Hulens, J. Verbeke, and T. Goedemé, "Choosing the best embedded processing platform for on-board UAV image processing," in *Proc. of the International joint conference on computer vision, imaging and computer graphics*. Springer, 2015, pp. 455–472.

[20] A. Charland and C. Clements, "Kinematic structure of a wildland fire plume observed by Doppler LiDAR," *IEEE/ACM Transactions on Networking*, vol. 118, no. 8, pp. 3200–3212, 2013.

[21] S. Boyd and L. Vandenberghe, *Convex Optimization*. New York, United States: Cambridge University Press, 2004.

[22] M. Mitchell, *An Introduction to Genetic Algorithms*. Cambridge, MA, USA: MIT Press, 1998.

[23] D. Beasley, D. R. Bull, and R. R. Martin, "An Overview of Genetic Algorithms: Part 2, Research Topics," *University Computing*, vol. 15, no. 4, pp. 170–181, 1993.

[24] X. Liu, X. Yu, and Z. Zhang, "PM2.5 concentration differences between various forest types and its correlation with forest structure," *Atmosphere*, vol. 6, no. 11, pp. 1801–1815, 2015.

[25] A. Alsharoa, H. Ghazzai, A. Kadri, and A. E. Kamal, "Spatial and temporal management of cellular hetnets with multiple solar powered drones," *IEEE Transactions on Mobile Computing*, vol. 19, no. 4, pp. 954–968, 2020.